Medical Radiology · Diagnostic Imaging
Series Editors: Hans-Ulrich Kauczor · Paul M. Parizel · Wilfred C. G. Peh

Marc Mespreuve
Karl Waked

MRI of the Wrist

A Practical Case-Based Approach

Springer

Medical Radiology

Diagnostic Imaging

The book series *Medical Radiology – Diagnostic Imaging* provides accurate and up-to-date overviews about the latest advances in the rapidly evolving field of diagnostic imaging and interventional radiology. Each volume is conceived as a practical and clinically useful reference book and is developed under the direction of experienced editors, who are world-renowned specialists in the field. Book chapters are written by expert authors in the field and are richly illustrated with high quality figures, tables and graphs. Editors and authors are committed to provide detailed and coherent information in a readily accessible and easy-to-understand format, directly applicable to daily practice.

Medical Radiology – Diagnostic Imaging covers all organ systems and addresses all modern imaging techniques and image-guided treatment modalities, as well as hot topics in management, workflow, and quality and safety issues in radiology and imaging. The judicious choice of relevant topics, the careful selection of expert editors and authors, and the emphasis on providing practically useful information, contribute to the wide appeal and ongoing success of the series. The series is indexed in Scopus.

Marc Mespreuve • Karl Waked

MRI of the Wrist

A Practical Case-Based Approach

Springer

Marc Mespreuve
Faculty of Medicine and Health Sciences
University of Ghent
Ghent, Belgium

Karl Waked
Plastic and Reconstructive Surgery
Free University of Brussels
Jette, Belgium

ISSN 0942-5373 ISSN 2197-4187 (electronic)
Medical Radiology
ISSN 2731-4677 ISSN 2731-4685 (electronic)
Diagnostic Imaging
ISBN 978-3-031-63972-2 ISBN 978-3-031-63973-9 (eBook)
https://doi.org/10.1007/978-3-031-63973-9

Preface

The idea for this project was initiated during the teaching courses as professor at the postgraduate medical education of the Department of Medical Imaging at the University of Ghent, Belgium (scientific chair Prof. Dr. K. Verstraete).

The need for a "pictorial essay of MRI of the wrist" in addition to the, albeit rare, up-to-date general textbooks seemed relevant. Not only colleagues who were less familiar with this specific topic showed interest but also residents in training and other interested radiologists and clinicians were fond of the proposed project.

The theoretical part of this book is limited to the essentials as are the references to additional literature. Therefore, the basic understanding and knowledge of osteoarticular MRI is needed to fully comprehend the illustrated pathologies.

The two major parts—traumatic pathology and non-traumatic pathology–are only based on the clinical presentation of the patients. There is, however, an overflow between both entities (e.g., repetitive microtrauma, acute trauma with non-traumatic underlying pathology, etc.).

The aim of this book is to provide an extra tool to the reader to take up the challenge of analysing in depth a wrist MRI by illustrating extensively not only the typical textbook pathology but also the less obvious and combined pathologies, which are displayed in different sequences.

Mostly, standard PA and lateral radiography views are added to allow a detailed comparison with the MRI images but also in the conviction that a wrist MRI exam should always be reported in conjunction with the available and less than 2-week-old standard views (at least four views: PA, lateral, clenched fist, and semi-pronated in ulnar deviation).

Sometimes, a case may be open for discussion…but that is also part of the goal of this book.

As "you only see what you know", it is important to realize that several anomalies may frequently be revealed, if searched for. One should certainly not be satisfied with finding the most obvious pathology. There may also be a disagreement between the MRI results and the initial clinical information. Therefore, a second consult with the clinician is part of the standard procedure in (complex) wrist pathology.

All the images in this book are real patient cases and were analysed and discussed in close collaboration with hand surgeons, orthopaedic surgeons,

and clinicians. Therefore, the description and diagnosis and the clinician's point of view are integrated throughout the selected images in this book.

Ghent, Belgium — Marc Mespreuve
Jette, Belgium — Karl Waked

Contents

Abbreviations

AP	AnteroPosterior
apl	abductor pollicis longus
AS	Abutment syndrome
ASC	ArthroSynovial cyst
AVN	Avascular necrosis
Ax	Axial
BMO	Bone marrow oedema
C	Capitate bone
cart	cartilage
CE	Contrast enhancement
CMC	CarpoMetaCarpal
Cor	Coronal
CPPD	Calcium pyrophosphate deposition disease
CT	Carpal tunnel
CTS	Carpal tunnel syndrome
DISI	Dorsal intercalated segment instability
dist	distal
dors	dorsal
DRUJ	Distal RadioUlnar joint
ecb	extensor carpi radialis brevis
ecl	extensor carpi radialis longus
ecu	extensor carpi ulnaris
ed	extensor digitorum
edm	extensor digiti minimi
epb	extensor pollicis brevis
epl	extensor pollicis longus
fcr	flexor carpi radialis
fcu	flexor carpi ulnaris
fd	flexor digitorum
fdp	flexor digitorum profundus
fds	flexor digitorum superficialis
FlR	flexor retinaculum
fpl	flexor pollicis longus
Gc	Guyon canal
H	Hamate bone
h	hamulus
I (-VI)	extensor compartment 1 (to VI)

IA	IntraArticular
L	Lunate bone
LT	LunoTriquetral
LTL	LunoTriquetral ligament
MC	MetaCarpal
MC-A	MidCarpal arthrography
MC-J	MetaCarpal joint
MedC-J	MedioCarpal joint
MH	Meniscus homologue
mn	median nerve
OA	OsteoArthritis
P	Pisiform bone
palm	palmar
(pl)	palmaris longus
pl	pollicis longus
PQ	Pronator Quadratus
PR	Prestyloid Recessus
prox	proximal
PsA	Psoriatic Arthritis
R Triq	Radiotriquetral ligament
R	Radius
ra	radial artery
RA	Rheumatoid arthritis
rad	radial
RCJ	Radiocarpal joint
RD	Radial deviation
rlt	radiolunotriquetral ligament
rsc	radioscaphocapitatum ligament
rul	radio-ulnar ligament
S Triq	Scaphotriquetral ligament
S	Scaphoid bone
Sag	Sagittal
SI	Signal intensity
SL	ScaphoLunate
SLL	ScaphoLunate ligament
(S)(O)CM	(Synovial) (Osteo)Chondromatosis
St	Styloid process
sup	superficial
T(ra)	Trapezium bone
t(ra)	trapezoid bone
T1WI	T1-Weighted Image
T1WI-FS	T1-Weighted Image Fat-Suppressed
T2WI	T2-Weighted Image
T2WI-FS	T2-Weighted Image Fat-Suppressed
TFC	Triangular FibroCartilago
TFCC	Triangular FibroCartilaginous Complex
TLis	Tuberculum of lister
Tra Triq	Trapeziotriquetral ligament

Tri	Triquetral bone
TriP	TriquetroPisiform
tub	tuberculum
U	Ulna
UA	Ulnar abutment
ua	ulnar artery
UCL	Ulnar collateral ligament
UD	Ulnar deviation
UL	Ulnolunate ligament
un	ulnar nerve
Utriq	Ulnotriquetral ligament

Part I

Section on Anatomy and Technique

Anatomy

Contents

The wrist is considered as the most complex anatomical and biomechanical structure in the human body (Loredo et al. 2005; MacLean et al. 2021). Hence, a thorough knowledge is essential.

The anatomy on MRI is usually easier to analyse in the axial plane on T1-weighted images fat-suppressed (T1WI-FS). The longitudinal continuity of a lot of structures helps their identification in the consecutive axial planes. Correlation with the coronal and sagittal plane can easily be achieved by positioning the 3D MRI cursor in the axial image(s).

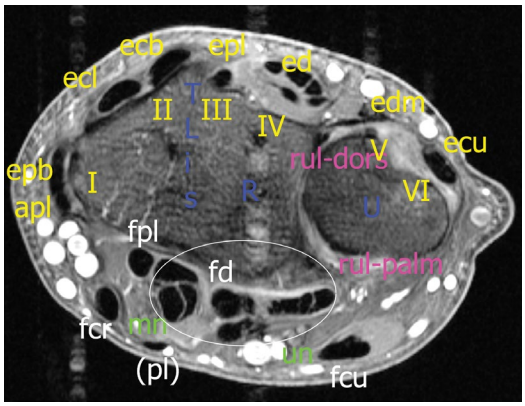

Fig. 1 Proximal cross-sectional view (Ax. T1-WI FS) at the level of the distal radius and ulna. Six dorsal extensor compartments numbered I to VI from radial to ulnar. The flexor tendons and median and ulnar nerves are illustrated at the palmar side of the wrist

1 Axial General MRI Anatomy

Starting proximally (Figs. 1 and 2) at the distal radius (R) and ulna (U), from radial to ulnar six extensor compartments—numbered I to VI—are delineated (Table 1).

M. Mespreuve, K. Waked, *MRI of the Wrist*, Medical Radiology,
https://doi.org/10.1007/978-3-031-63973-9_1

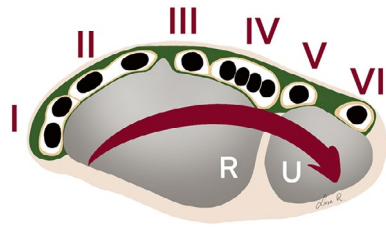

Fig. 2 The extensor retinaculum (green). The retinaculum subdivides the extensor region in six compartments (I-VI) and holds the tendons on-site. (Illustrated by Lisa Ramaut, MD)

Table 1 Extensor compartments of the wrist

Compartment	Tendon(s)	Abbreviation
I	Abductor pollicis longus Extensor pollicis brevis	apl epb
II	Extensor carpi radialis longus Extensor carpi radialis brevis	ecl ecb
III	Extensor pollicis longus (variable position II-IV)	epl
IV	Extensor digitorum	ed
V	Extensor digiti minimi	edm
VI	Extensor carpi ulnaris	ecu

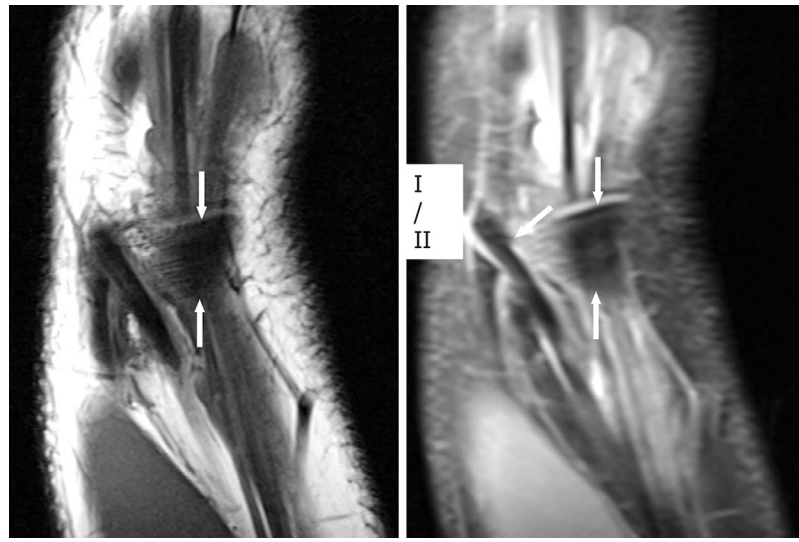

Fig. 3 The extensor retinaculum (Cor T1-WI and T2 WI-FS). The low signal band of the extensor retinaculum at the level of the (proximal) crossover of the tendons of compartment I over II (radially)

The extensor tendons are held in place by the extensor retinaculum, surrounding the tendons and subdividing the extensor region (Fig. 2). On the coronal images, the extensor retinaculum may be seen as a low signal band at the (proximal) crossover of the tendons of compartment I over II (Fig. 3).

An important dorsal landmark is the tuberculum of Lister (TLis) (Bhat et al. 2011)

The palmar tendinous structures from radial to ulnar are the flexor carpi radialis (fcr), the flexor pollicis longus (fpl), the flexor digitorum (fd), and the flexor carpi ulnaris (fcu).

The palmaris longus (pl) is inconsistently present centrally and most superficial (running over the flexor retinaculum).

Two important nerves must be delineated as well: the median nerve (mn) runs at the radial side between the fcr (superficial) and the fpl and fd (deep); the ulnar nerve (un) runs medially between the fd (deep) and fcu (superficial).

At the distal radio-ulnar joint (Ekenstam and Hagert 1985; Nakamura 2012; Schmitt et al. 2003), the dorsal and palmar radio-ulnar ligaments (rul) are noted.

More distally (Fig. 4), the triangular fibrocartilage (TFC) appears between the radial notch and the ulnar styloid process (St). The radial (ra) and ulnar (ua) arteries may be delineated between multiple venous structures at the radial side of respectively the median (mn) and ulnar (un) nerve.

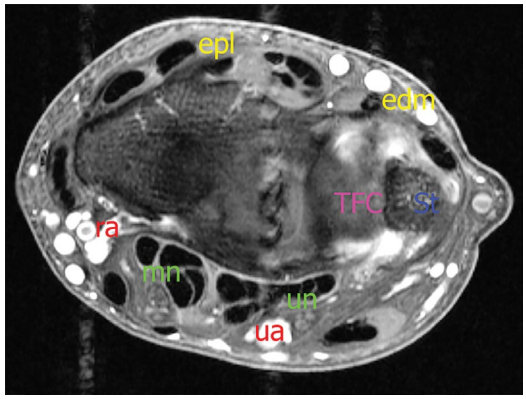

Fig. 4 The triangular fibrocartilage (Ax. T1-WI FS). The TFC appears between the radial notch and the ulnar styloid process (St). The radial and ulnar arteries are located at the radial side of respectively the median (mn) and ulnar (un) nerve

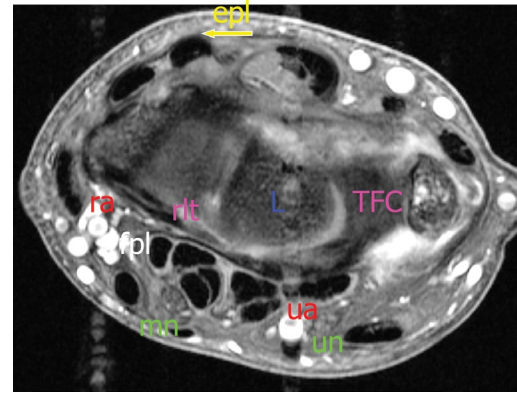

Fig. 5 The level of the proximal pole of the lunate bone (Ax. T1-WI FS). Dorsally, the distal crossover of the epl and at the palmar side the radial part of the palmar extrinsic radiolunate ligament appears at the level of the proximal pole of the lunate bone

The proximal pole of the lunate carpal bone (L) appears (Fig. 5) centrally, as does the radial part of the palmar extrinsic radiolunate ligament (rlt). At the dorsal side, the extensor pollicis longus tendon (epl; III) starts crossing over the tendons of compartment II (distal crossover).

The bones of the proximal carpal row (scaphoid (S), lunate (L), and triquetral (Tri) bone) are delineable, with the intrinsic ligaments (scapholunate (sl), lunotriquetral (lt)) running between them, as well as the palmar extrinsic radiolunate ligament (rlt) (Figs. 6 and 7). The ulnar snuff box is an anatomical landmark at the ulnar side between the ulnar flexor and extensor tendons.

At the level of the triquetropisiform joint (Fig. 8), which is located at the entrance of the carpal tunnel, the lunate bone is positioned between a part of the palmar radio-scapho-capitate (rsc) and the radiolunate (rlt) ligament. The median nerve is situated very superficially, under the proximal part of the flexor retinaculum (Fl R). The triangular Gyon canal (Gc) has its base against the pisiform bone and the flexor retinaculum at its bottom. Consequently, the ulnar artery and nerve are isolated from the carpal tunnel at this level. The flexor carpi ulnaris (fcu) tendon inserts on the pisiform bone. Dorsally, an ulnar part of the extrinsic radio-triquetral ligament (rtriq) appears.

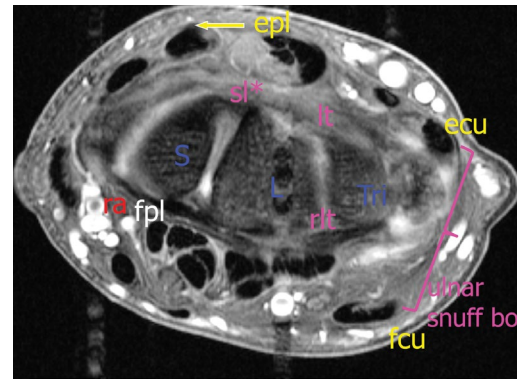

Fig. 6 The proximal carpal row (Ax. T1-WI FS). The bones of the proximal carpal row composed of the scaphoid (S), lunate (L), and triquetral (Tri) bone. The intrinsic ligaments (scapholunate (sl), lunotriquetral (lt)) are running between them. The ulnar part of the palmar extrinsic radiolunate ligament (rlt) is noted as is the ulnar snuff box

The proximal pole of capitate bone (C) is now centrally located (Fig. 9) and the carpal tunnel fully extended. The radial artery (ra) moves radio-dorsally.

Moving further on (Figs. 10 and 11) to the proximal part of the distal carpal row (Bonnel and Allieu 1984) (formed by the trapezoid (tra) and hamate (H) bone), the median nerve (mn) continues its superficial trajectory under the distal part of the flexor retinaculum. At the radial side, the radial snuff box—another important

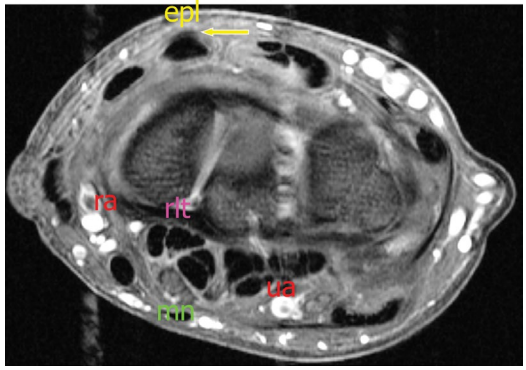

Fig. 7 The proximal carpal row (more distally) (Ax. T1-WI FS). The radial part of the palmar extrinsic radiolunate ligament (rlt)

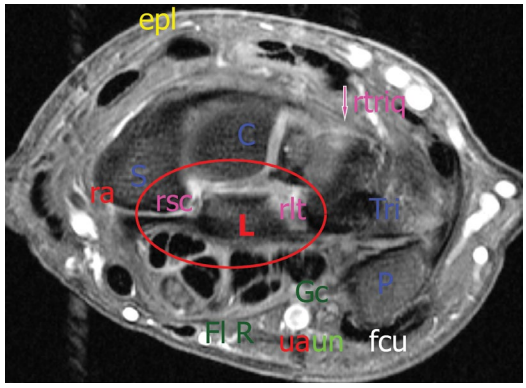

Fig. 8 Entrance of the carpal tunnel (Ax. T1-WI FS). At the level of the triquetropisiform joint (Tri-P), the L is positioned between a part of the palmar radioscaphocapitate (rsc) and the radiolunate (rlt) ligament. The median nerve is situated superficially, under the flexor retinaculum (Fl R). The triangular Gyon canal (Gc) has its base against the pisiform bone with the flexor retinaculum at its bottom and contains the ulnar artery and nerve. Dorsally, an ulnar part of the extrinsic radio-triquetral ligament (rtriq) appears

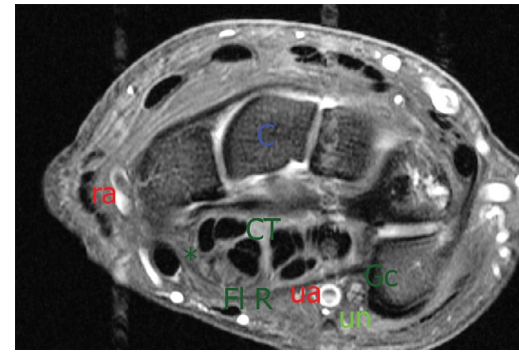

Fig. 9 The carpal tunnel (Ax. T1-WI FS). The proximal pole of capitate bone (C) is centrally located. The radial artery (ra) moves radio-dorsally

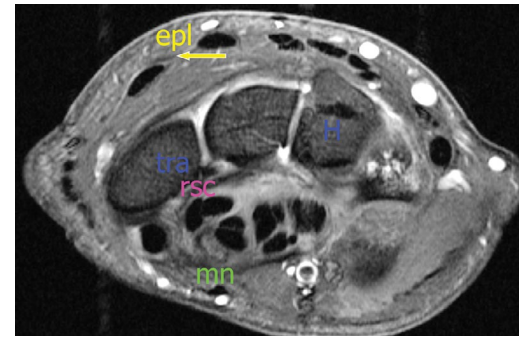

Fig. 10 Proximal part of the distal carpal row (Ax. T1-WI FS). The proximal part of the distal carpal row formed by trapezoid (tra) and hamate (H) bone). The median nerve (mn) continues its superficial trajectory

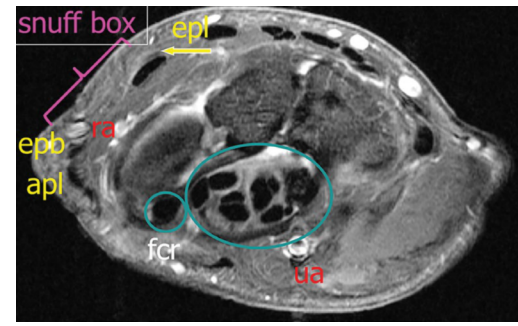

Fig. 11 The distal carpal row (Ax. T1-WI FS). The radial snuff box is bordered by the epl (medially) and the epb and apl (laterally). The radial artery is situated dorsally and runs along the floor of the snuff-box

anatomical landmark—is noted, bordered by the epl (medially) and the epb and apl (laterally). Meanwhile, the radial artery is situated dorsally and runs along the floor of the snuff box. The flexor carpi radialis (fcr) is separated from the other flexor tendons and runs closely to the tuberculum of the trapezium bone (Tra) (Fig. 12). The deep flexor tendons are more separated from the superficial tendons and located at the bottom of the carpal tunnel. The carpal tunnel thus contains all four superficial and deep flexor digitorum tendons, as well as the flexor pollicis longus, located most laterally and superficial to the scaphoid bone (S). The ulnar nerve passes superficial from

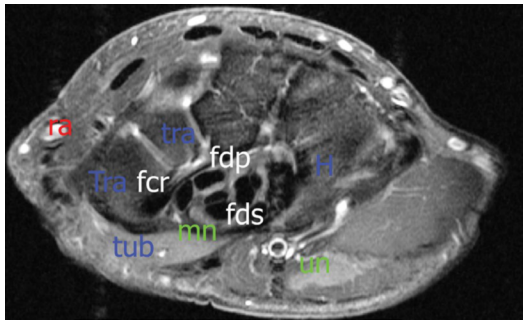

Fig. 12 The distal carpal row at the level of the tuberculum (tub) (Ax. T21-WI FS). The flexor carpi radialis (fcr) is separated from the other flexor tendons and runs closely to the tuberculum of the trapezium bone (Tra). The deep flexor tendons are more separated from the superficial tendons and located at the bottom of the carpal tunnel

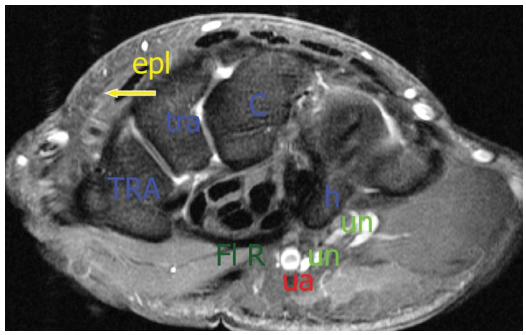

Fig. 13 The distal carpal row at the level of the hamulus (h) (Ax. T21-WI FS). The ulnar nerve passed between the pisiform bone (lateral) and the hamulus (medial) and splits in a superficial and deep branch. The deep branch of the ulnar nerve accompanies the deep branch of the ulnar artery

the flexor retinaculum, between the pisiform bone (lateral) and the hamulus (medial) and splits in a superficial and deep branch (Figs. 13 and 14). Interestingly, the deep branch of the ulnar nerve accompanies the deep branch of the ulnar artery.

The four distal carpal row bones (trapezium (TRA), trapezoid (tra), capitate (C), and hamate with the hamulus (h)) form the distal part of the bony carpal tunnel (Fig. 13), limited at the palmar side by the flexor retinaculum (Fl R). The two branches of the ulnar nerve (un) are situated superficially and at the ulnar side of the hamulus (Figs. 13 and 14) and give rise to a deep dorsal

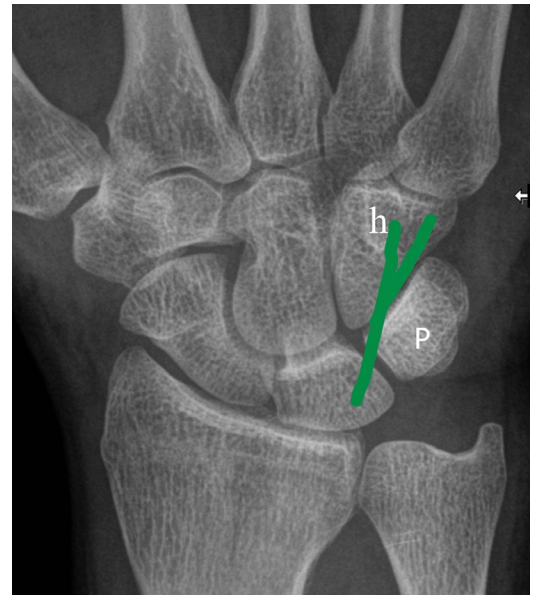

Fig. 14 Schematic drawing of the ulnar nerve trajectory. The ulnar nerve passes between the pisiform bone (laterally) and the hamulus (medially) and splits in a superficial and deep branch

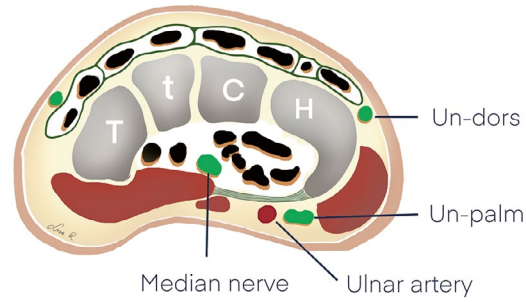

Fig. 15 Schematic drawing of the nerves at the level of the hamulus. The deep dorsal (un-dors) and superficial palmar branch (un-palm) of the ulnar nerve. (Illustrated by Lisa Ramaut, MD)

(un-dors) and superficial palmar branch (un-palm) (Fig. 15).

The bases of the metacarpals (Gunther 1984; Nakamura et al. 2001a; Theumann et al. 2002; Zancolli et al. 1987) appear (Figs. 16, 17, and 18), while the epl continues its crossing course. The median nerve is splitting into 5–6 components, while a superficial palmar branch runs superficially from the flexor retinaculum as does

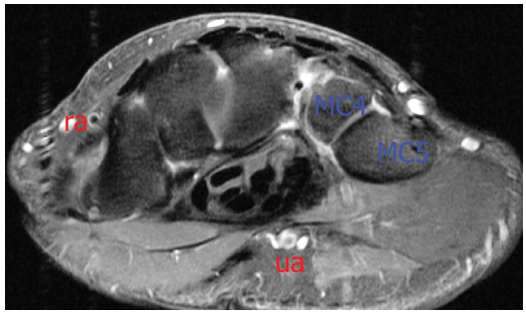

Fig. 16 The bases of the ulnar metacarpals (Ax. T1-WI FS). The bases of the metacarpals appear

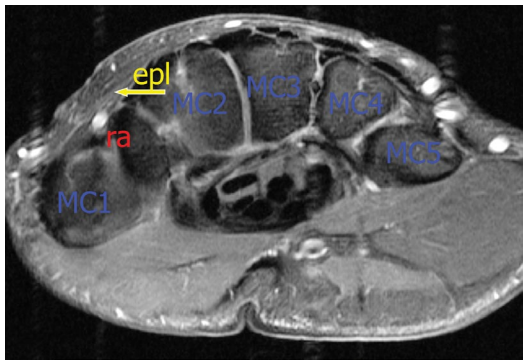

Fig. 17 The bases of the metacarpals (Ax. T1-WI FS). The epl continues its crossing course

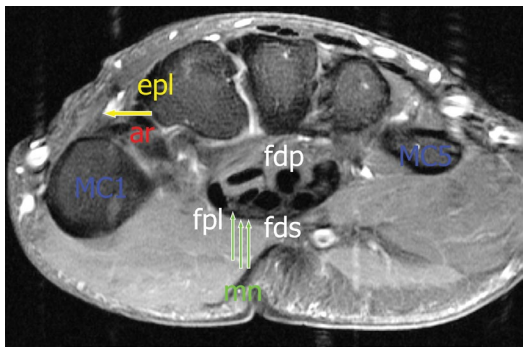

Fig. 18 The proximal metacarpals (Ax. T1-WI FS). The median nerve is splitting into 5–6 components

a recurrent superficial branch (Fig. 19), which in normal conditions are difficult to distinguish.

T2-weighted images fat-suppressed (T2WI-FS) may be useful in identifying specific structures due to the internal fascicular signal of the small ulnar nerve and the flow void of the

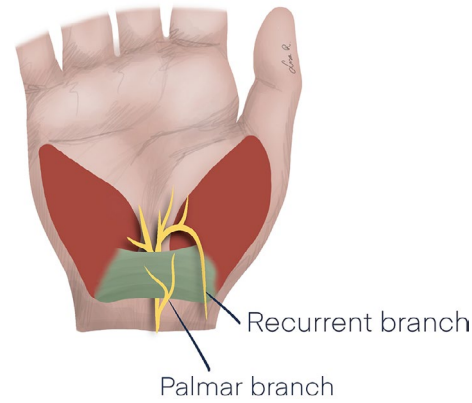

Fig. 19 Schematic drawing of the two important branches of the median nerve. The superficial palmar branch runs superficially from the flexor retinaculum as does a recurrent superficial branch. (Illustrated by Lisa Ramaut, MD)

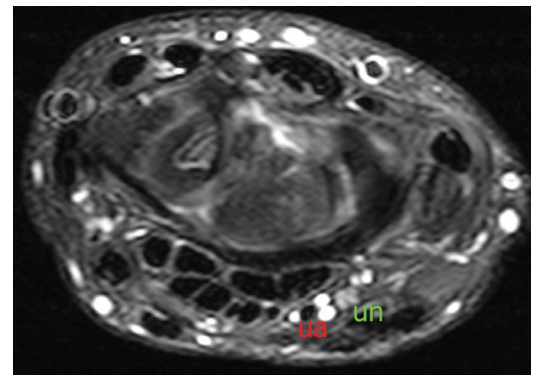

Fig. 20 The ulnar nerve (Ax. T2-WI FS). The internal fascicular signal of the small ulnar nerve

ulnar artery (Figs. 20, 21, 22, 23, and 24). The virtual Parona space (Fig. 25) (a "highway" between the forearm and the hand, located between the Pronator Quadratus muscle (deep) and fdp (superficial), and just proximal to the carpal tunnel) and the potential presence of liquid (pathognomonic for a horse shoe abscess), the separation between the fcr (Fig. 26) and the rest of the flexor tendons of the carpal tunnel and the patency of vascular structures (Fig. 27) is better illustrated.

For the exact delineation of the joint capsule (containing the extrinsic ligaments) versus the overlying tendons, an arthrography technique is needed (Fig. 28).

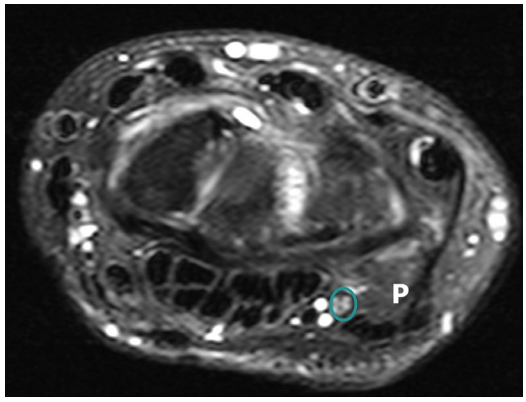

Fig. 21 The ulnar nerve continued (Ax. T2-WI FS). The higher signal of the small ulnar nerve at the level of the P

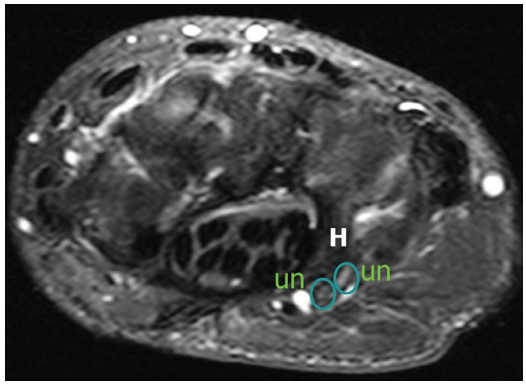

Fig. 22 The ulnar nerve continued (Ax. T2-WI FS). The higher signal of the small ulnar nerve branches at the level of the hamulus

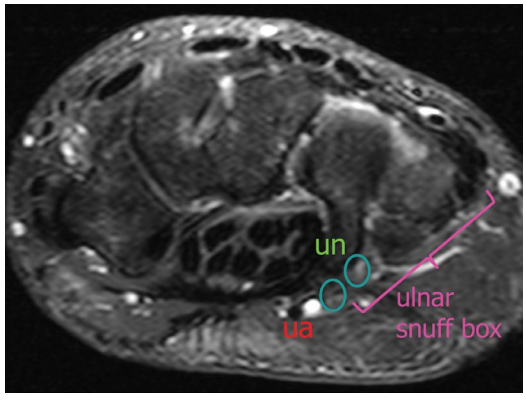

Fig. 23 The ulnar artery (Ax. T2-WI FS). Flow void of the ulnar artery

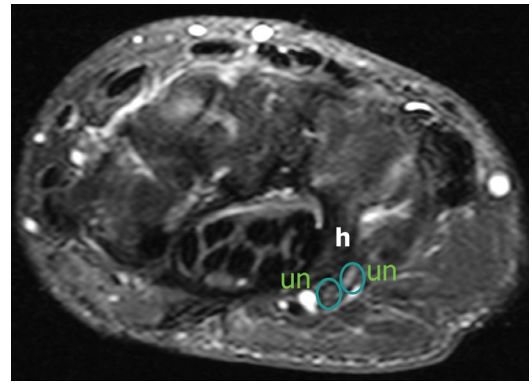

Fig. 24 The ulnar nerve continued (Ax. T2-WI FS). Splitting of the ulnar nerve, higher signal with fascicules

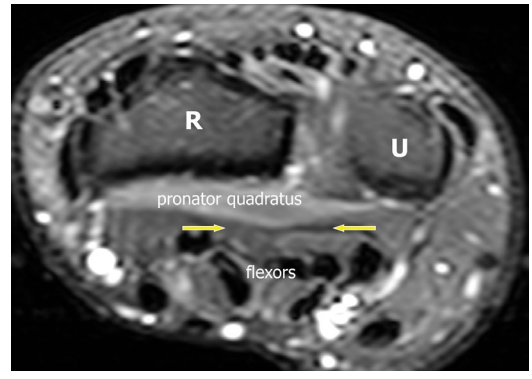

Fig. 25 The virtual space of Parona (Ax. T2-WI FS)

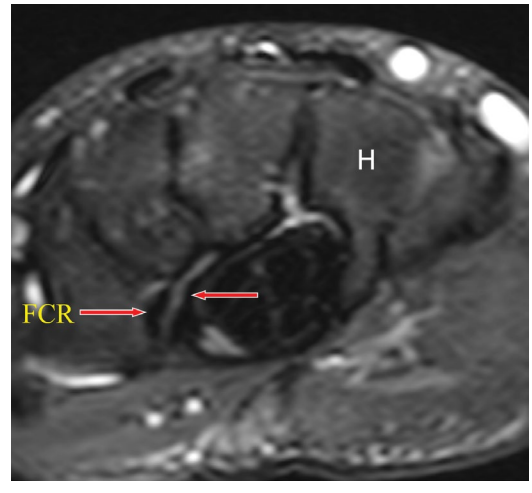

Fig. 26 (Ax. T2-WI FS). There is a clear separation between the fcr and the rest of the flexor tendons

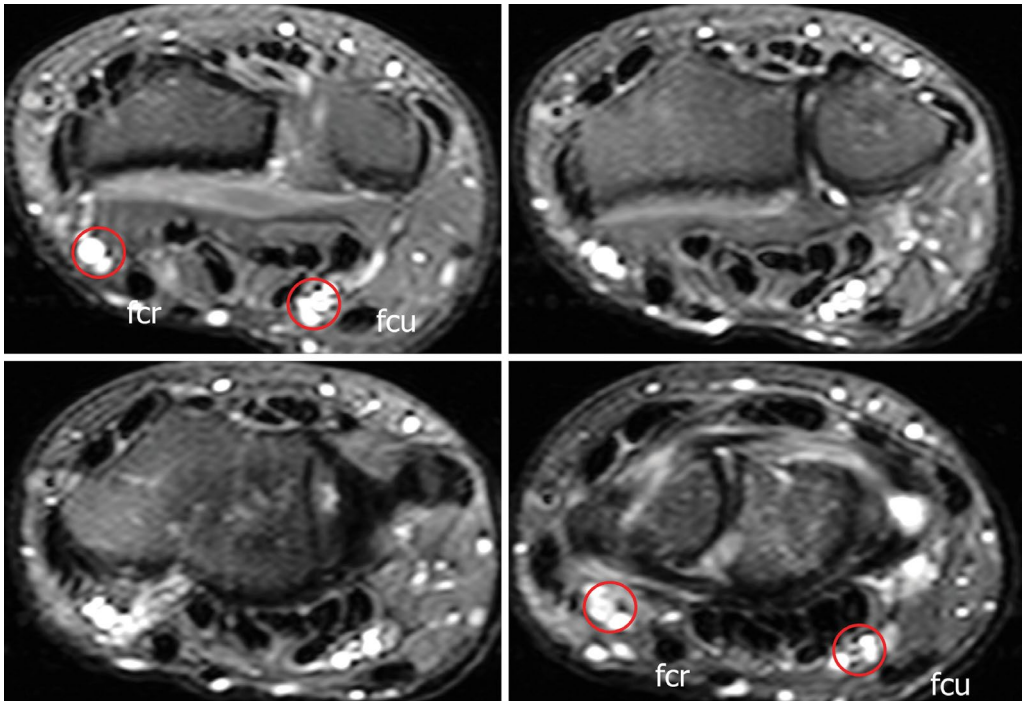

Fig. 27 Ax. T2-WI FS at several locations. Homogenous high signal on the trajectory of the arteries

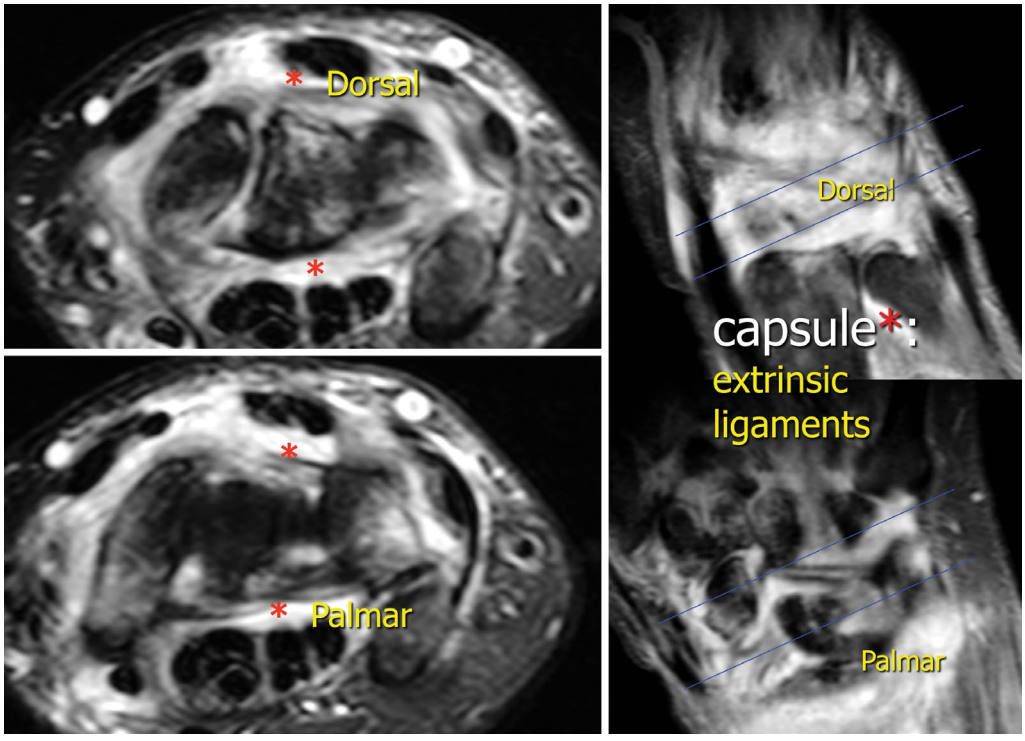

Fig. 28 MR arthrography (Ax. and Cor T2-WI FS). Visualization of the joint capsule (Ax) containing the extrinsic ligaments (Cor)

2 Ligaments

A lot of ligamentous structures (MacLean et al. 2021; Boutry et al. 2005; Davis and Blankenbaker 2010; Gitto and Draghi 2016; Gitto et al. 2017; Pulos and Bozentka 2015; Ringler 2013; Ringler and Murthy 2015; Scheck et al. 1999; Zlatkin and Rosner 2006) form connections between the carpal bones (intrinsic ligaments) as well as connections between the carpal and adjacent bones (extrinsic ligaments). Optimally, axial images are combined with coronal and/or sagittal images to visualise the complex trajectory of these ligaments.

2.1 Intrinsic Ligaments

The bones of the distal carpal row are connected by firm intrinsic (Lee et al. 2017; Manley et al. 2013; Schmid et al. 2005; Sennwald et al. 1994; Zdravkovic et al. 1994) interosseous ligaments (trapeziotrapezoid, capitotrapezoid, and capitohamate ligament) (Fig. 29). These limit the midcarpal joint distally, although there is a connection with the carpo-metacarpal joint (M-joint) through the central interruption of the trapeziotrapezoid ligament (Figs. 30 and 31). The distal extensions of the M-joint between the metacarpal bases II–V are limited by the intermetacarpal ligaments

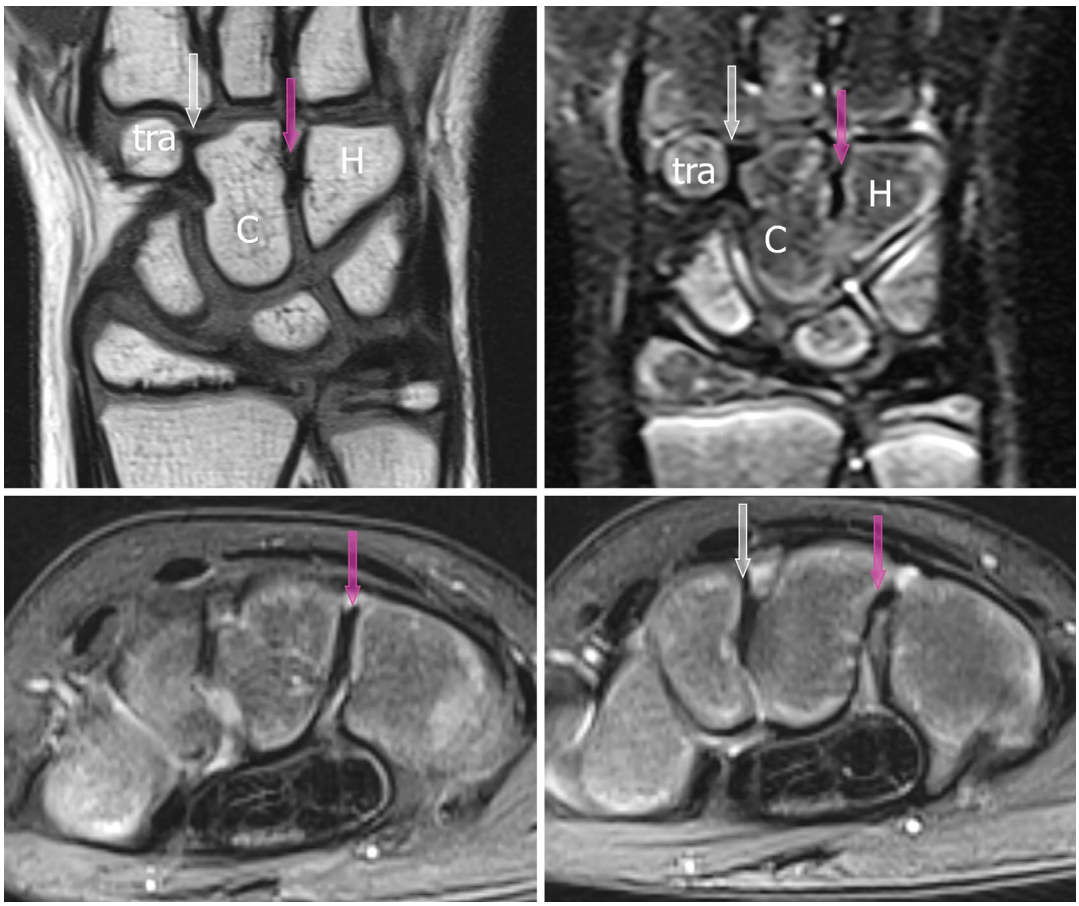

Fig. 29 The capitotrapezoid (white) and capitohamate (pink) ligament of distal carpal row (Cor T1-WI, T2-WI FS, and Ax T1-WI FS)

(Fig. 31). Special attention must be given to the variable configuration of the quadrangular joint (Figs. 32 and 33).

The capsular borders of the dorsal side of the CMC-joint are in close contact with the tendon insertions of the extensor carpi radialis longus and brevis, respectively, at the dorsal side of the base of MC II and III (Fig. 34).

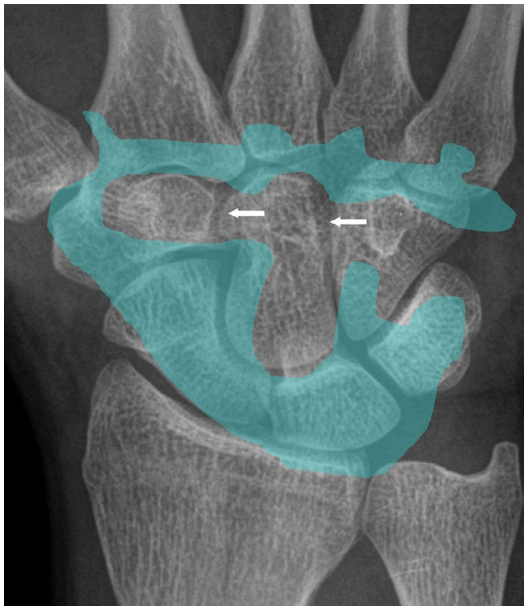

Fig. 30 Schematic drawing of the midcarpal arthrogram. No contrast passing (arrows) through the capitotrapezoid and capitohamate ligament of distal carpal row

The scapholunate (SL) and lunotriquetral (LT) intrinsic ligaments of the proximal carpal row are essential structures for the wrist motion. The scapholunate ligament (Shahabpour et al. 2015) mostly presents centrally as a triangular structure situated proximally between the scaphoid and lunate bone (Fig. 35). However, its form changes as the ligament has a horseshoe or C-shaped aspect in the sagittal plane. The ligamentous attachment to the adjacent bones varies. The central part attaches to the cartilage, whereas the dorsal and ventral parts attach to the cortex of the scaphoid bone and by Sharpey fibres to the lunate bone (Fig. 36). The most important dorsal part (Fig. 37), due to its C-shaped configuration, seems to extend between the carpal bones (Figs. 36 and 37). In children, the ligament is situated more eccentric in the SL bony space due to the remaining presence of a large cartilaginous part at the proximal pole of the scaphoid bone (Fig. 38). Midcarpal arthrography (Fig. 39) shows the exact location and continuity of the SL. The lunotriquetral ligament (Ritt et al. 1998) is smaller and mostly bandlike or triangular (Figs. 40, 41, and 42). The form also changes as the ligament has a similar horseshoe shape in the sagittal plane.

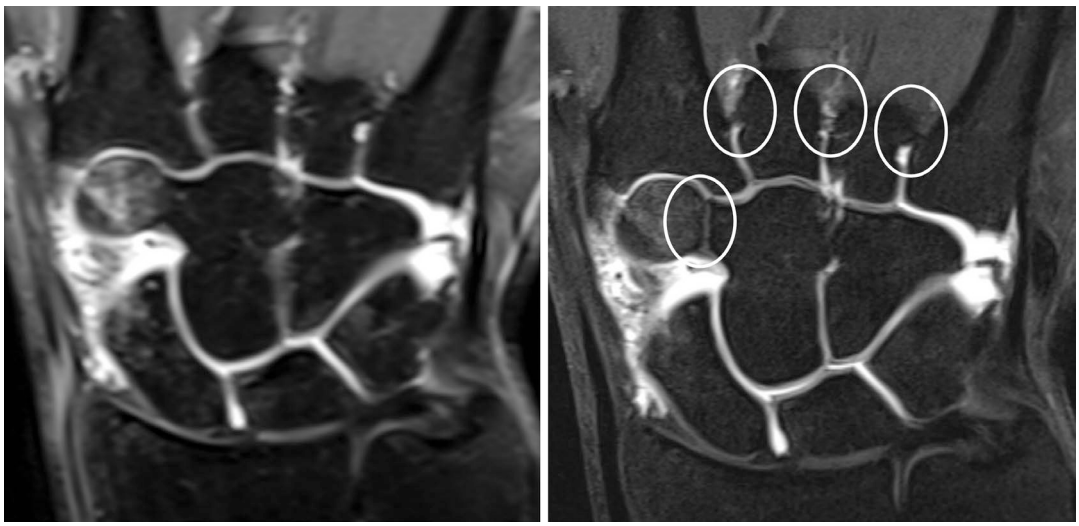

Fig. 31 Midcarpal Cor T1-WI FS arthrography. The midcarpal joint is in normal communication with the M-joint through the Tra-tra space. The intermetacarpal spaces are distally limited by small ligaments

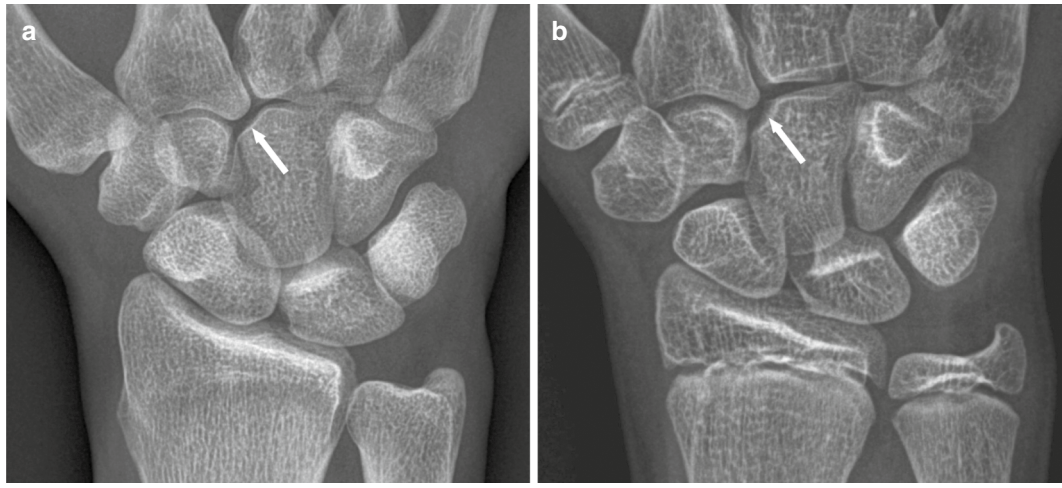

Fig. 32 Standard PA view. The quadrangular space in adult (**a**) and child (**b**)

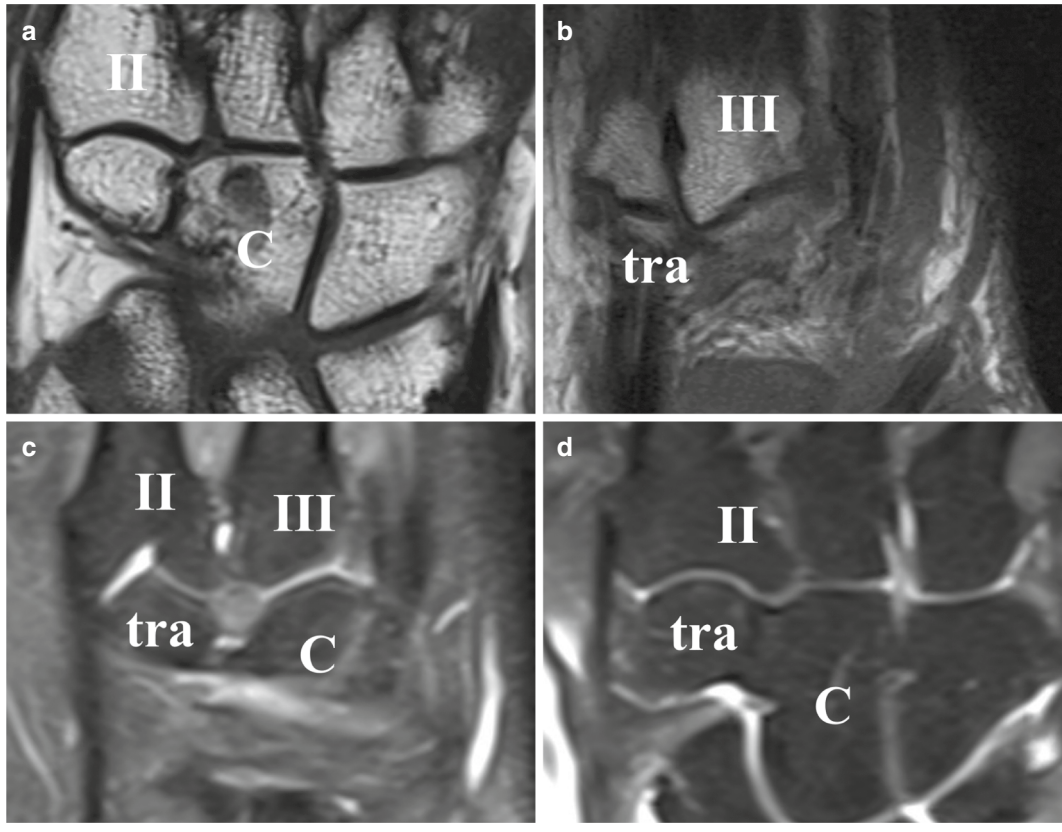

Fig. 33 Cor T1-WI (**a**, **b**) and Cor T2-WI FS (**c**, **d**). Variable configurations of the quadrangular joint: MC II—C contact (**a**); MC III—tra contact (**b**); interposition of styloid bone between MC II, III, tra and C (**c**) and coalition tra-C in contact with MC II (**d**)

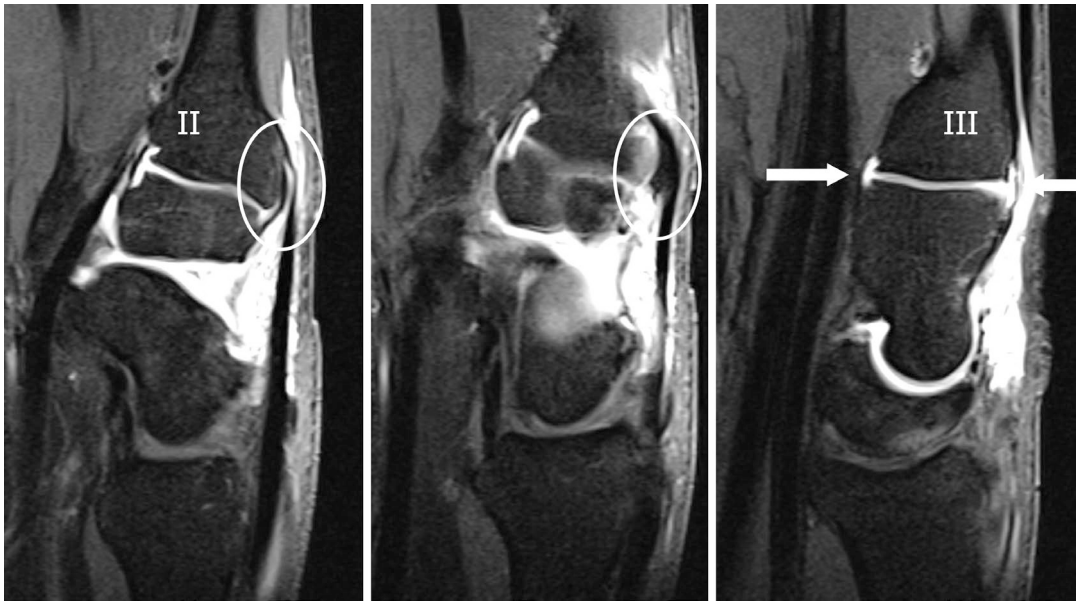

Fig. 34 MR GRE arthrography. Close contact between the insertion tendons of the ecl and ecb and, respectively, the dorsal capsule of the MC II and MC III joint (ovals). Contrast in the MC joints limited by the ventral and dorsal part of the capsule (arrows)

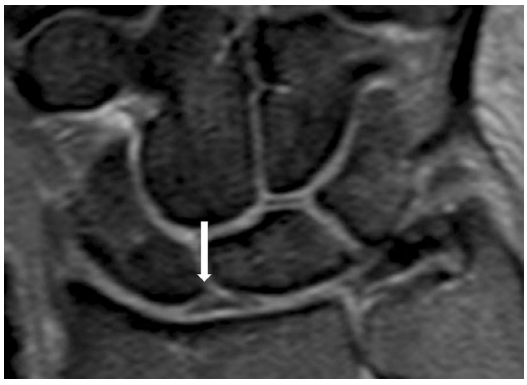

Fig. 35 Cor T2-WI FS. A triangular homogenous low signal SL is proximally positioned between the S and L

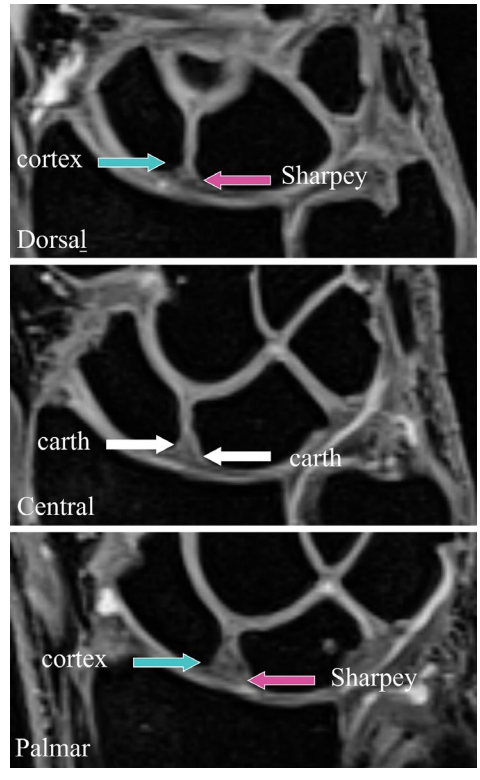

Fig. 36 Cor GRE. The ligament is attached to the ventral and dorsal cortex on the S side and by Sharpey fibers on the L side. Centrally it is fixated on the cartilage

The ligamentous attachment to the adjacent bones varies (Fig. 41). The most important part is the palmar component (Fig. 41).

Although the triangular fibrocartilaginous complex (TFCC) (Nakamura et al. 2001b; Zhan et al. 2020) (Fig. 43) is not an intrinsic ligament, it is often mentioned together with the SL and LT. This complex structure contains seven components, which are summarised in Table 2. A small cartilage band is interposed (Fig. 44) between the radial notch and the triangular

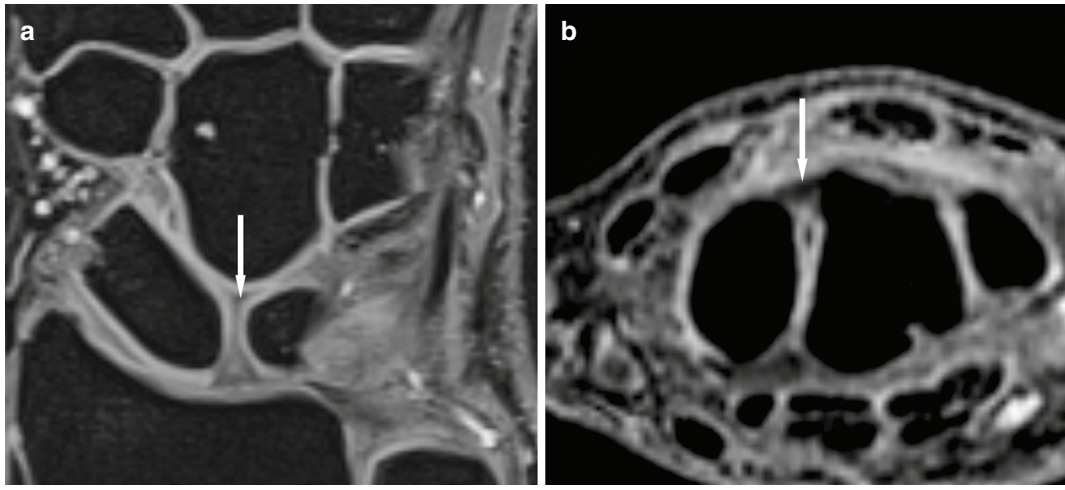

Fig. 37 Cor (**a**) and Ax (**b**) GRE. The dorsal part of the SL (arrows) is the most important part

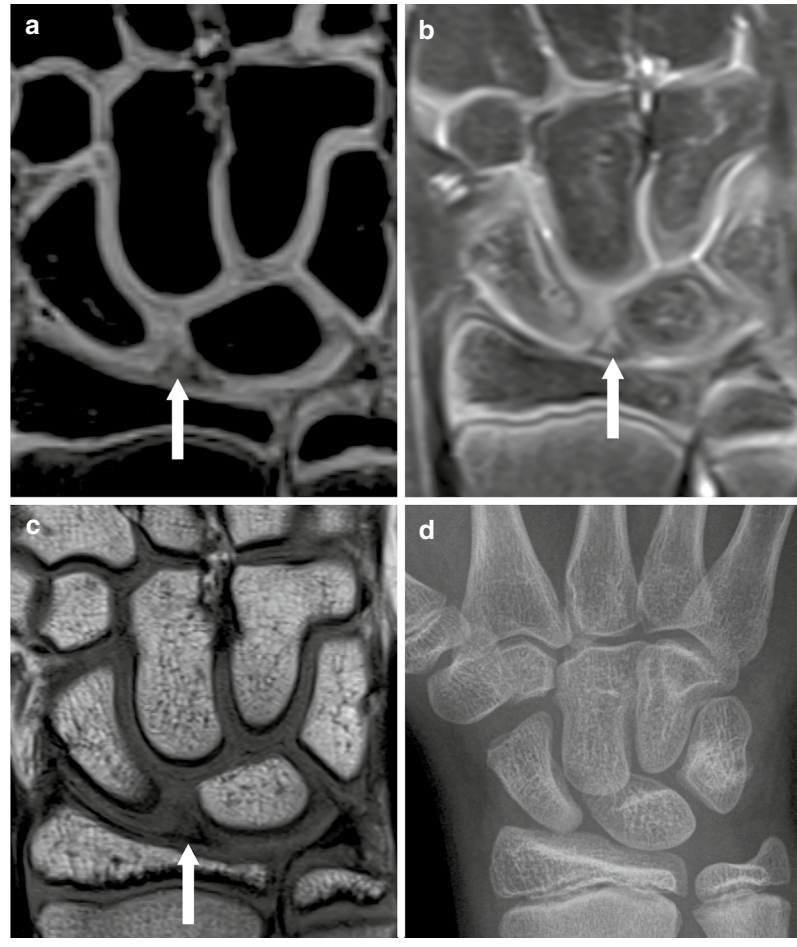

Fig. 38 Cor GRE (**a**), proton density (**b**), T1-WI (**c**) imaging and standard PA view (**d**). Pseudo-widening of the SL joint space and eccentric position of the low signal ligament (arrows) in the SL bony space due to a large still cartilaginous part of the proximal pole of the scaphoid bone in a child

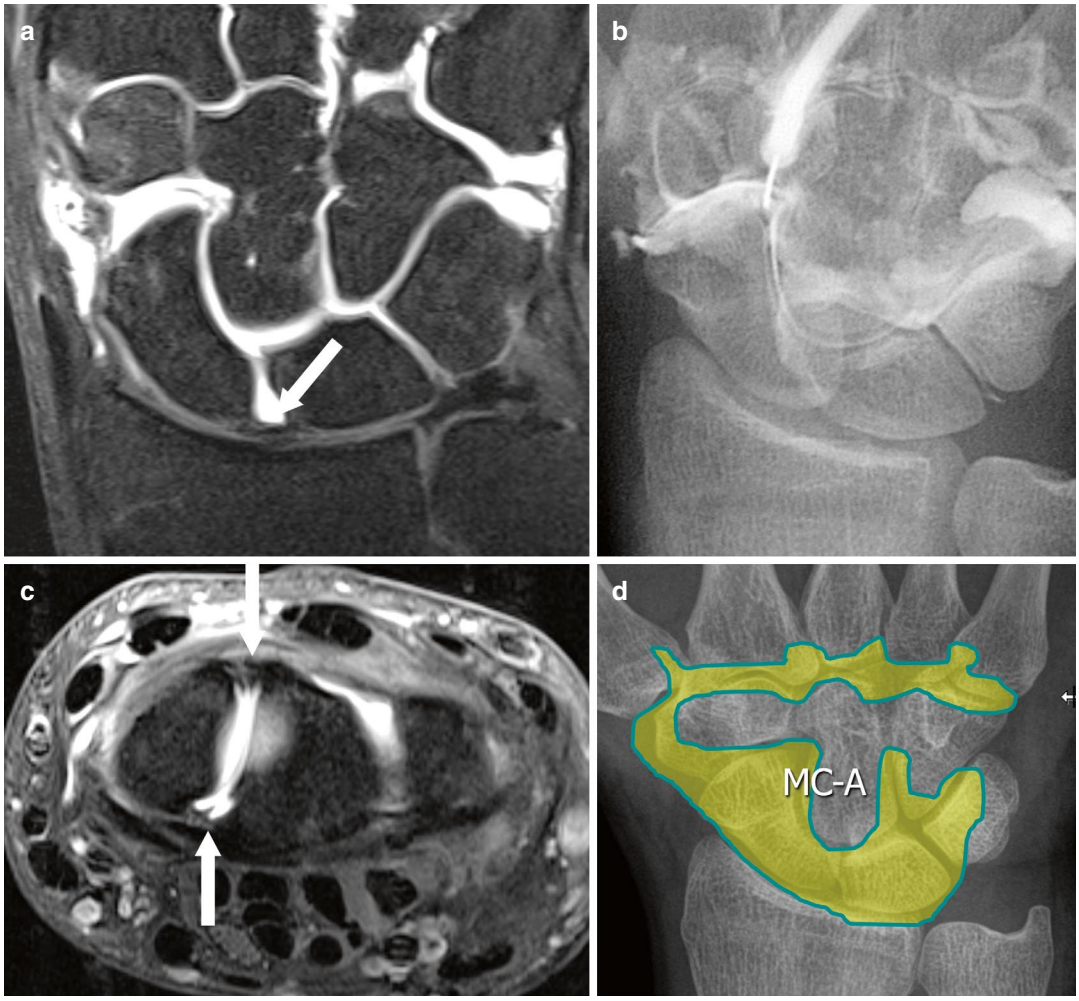

Fig. 39 Midcarpal arthrography Cor and Ax T1-WI FS (**a**, **b**), standard PA arthrography view (**c**) with schematic drawing of MCA (**d**). The space between the S and L is opacified by contrast and delineates the distal border of the SL. The interpretation of the continuity needs at least coronal (**a**) and axial (**b**) images. The observation during the injection and the arthrography views (**c**, **d**) are an integral part of the examination

structure. The poorly vascularised central disc has a well vascularised double insertion on the ulnar styloid process near the base (ulnar notch) and near the tip (Figs. 43a, 44a, and 45a). The TFCC separates the radiocarpal joint (RCJ) from the distal radio-ulnar joint (DRUJ) (Fig. 43b) and provides stability to the latter joint. The base of the meniscus homologue (Figs. 43b and 45b) rests on the ulnar collateral ligament and delineates the entrance to the pre-styloid capsule recessus of the radiocarpal joint (Fig. 45c, d). At the palmar and dorsal side, the radio-ulnar ligament maintains the position of the ulnar head in the radial notch (Fig. 46a). Two small palmar ligaments connect the TFCC and the palmar radio-ulnar ligament to the lunate (ulnolunar) and triquetral (ulnotriquetral) bones (Fig. 46b, c).

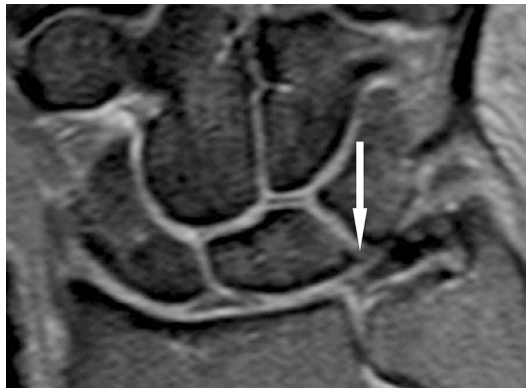

Fig. 40 Cor T2-WI FS. A bandlike homogenous low signal LT is proximally positioned between the L and Tri

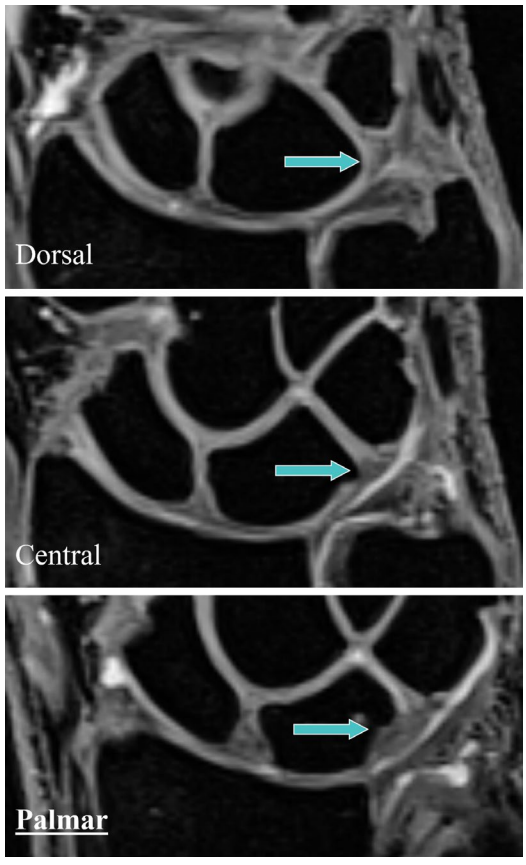

Fig. 41 Cor GRE. The form of the LT changes and the palmar component is the strongest of the three parts

Rarely mentioned ligaments are the intrinsic ligament between the trapezium and scaphoid bone (Fig. 47) as well as those between the hamate and triquetrum proximally and the base of the fifth metacarpal distally (Fig. 48).

2.2 Extrinsic Ligaments

To achieve a clear and structured approach, the extrinsic ligament (Shahabpour et al. 2011) nomenclature is derived from their bony insertion points. Most of them run in an oblique 3D-direction and thus need to be evaluated on successive images.

2.2.1 Palmar Side

On MRI images, two V-shaped structures are considered (Figs. 49, 50, 51, 52, 53, 54, and 55). Distally, the V located on the radial side is formed by the radioscaphocapitate ligament (1), continuing on the ulnar side as a proximal (5a) and distal (5b) part of the scaphocapitate-triquetral ligament (5; Prendergast ligament). Proximally, the radial component of the V is formed by the radiolunotriquetral ligament (2). The ulnar component consists of the small ulnolunar (3) and ulnotriquetral (4) ligaments.

The sometimes-mentioned deltoid ligament refers to the radioscaphocapitate ligament continued by the scaphocapitate-triquetral ligament (Fig. 54).

At the radial side, the space of Poirier is situated between the radioscaphocapitate (1) and radiolunotriquetral (2) ligament (Fig. 50).

The classical "palmar V" is composed of (1), (2), and (5) (Fig. 49).

Obermann (1991) first introduced the term "proximal palmar V" ((2), (3) and (4)) (Fig. 49).

A fairly large number of the ligaments form a central fixed column (T-form, formed by the distal carpal row and the L) (Fig. 54b). The radial (S) and ulnar columns (Tri) allow for the carpal mobility.

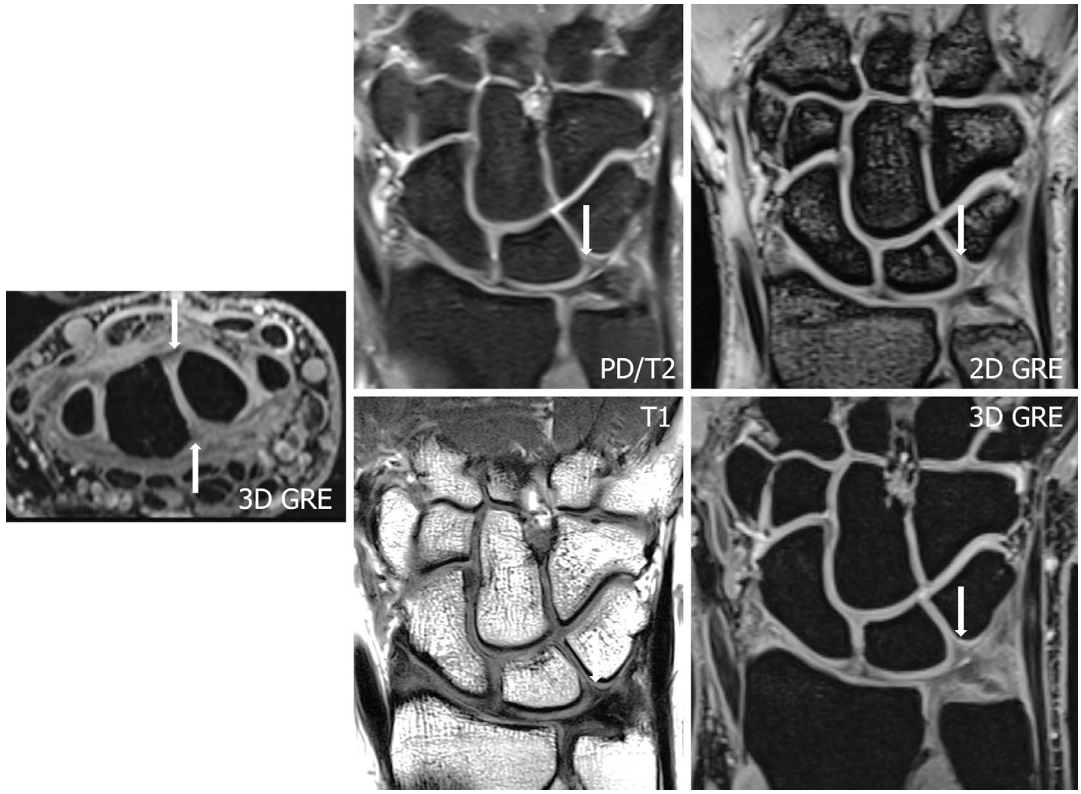

Fig. 42 Different imaging sequences of the LT. The form, signal, and continuity should be evaluated in two orthogonal dimensions

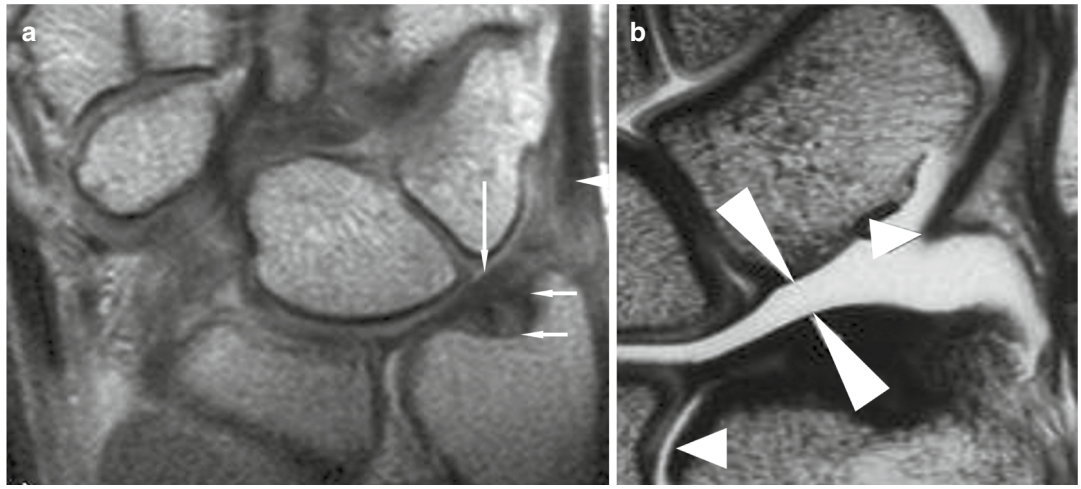

Fig. 43 T1-WI (**a**) and MR-arthrography (**b**). The TFCC (A-Ad) has a double insertion on the ulnar styloid (A-double Alr). It separates the RCJ (B-double AH) from the DRUJ (B-Ahr). The meniscus homologue (B-Ahl) rests on the ulnar collateral ligament (A-Ahr)

Table 2 Components of the TFCC-complex

Components		Abbreviation
Triangular fibrocartilage	Central articular disc	TFC-AD
Double ulnar attachment	Tip of the styloid ulnar notch	
Palmar and dorsal radio-ulnar ligament		rul (palm/dors)
Meniscus homologue		MH
Ulnar collateral ligament		UCL
Ulnocarpal ligaments	Ulnolunate and ulnotriquetral	UL and Utriq
Tendon sheath of extensor carpi ulnaris		ecu

2.2.2 Dorsal Side

The main ligaments converge to the dorsum of the triquetral bone (Figs. 56 and 57). Their origin is located, respectively, on the radius (1), the scaphoid (2), and the trapezium (3) bone. The often-used term "dorsal intercarpal ligament" refers to (1) and (2).

The ulnotriquetral (4) and the radial collateral ligaments (5) can also be visualised. Note that (2) and (3) are connecting carpal bones and should theoretically be considered as "intrinsic".

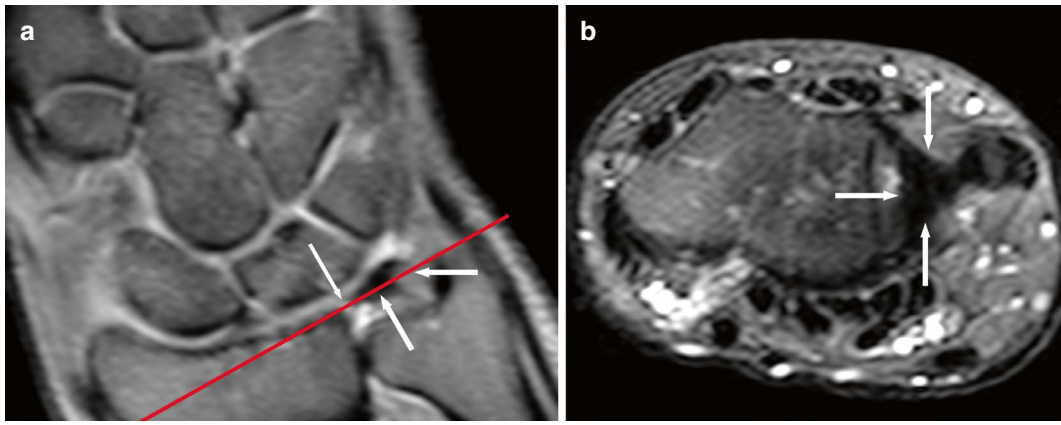

Fig. 44 Cor proton density (**a**) and Ax T2-WI FS (**b**) (at the level of the red line in **a**). There is a small band at the radial sigmoid notch (A-AOdl) between the central disc (A-AOar, B-arrows) and the highly vascularized ulnar insertion (A-Alr)

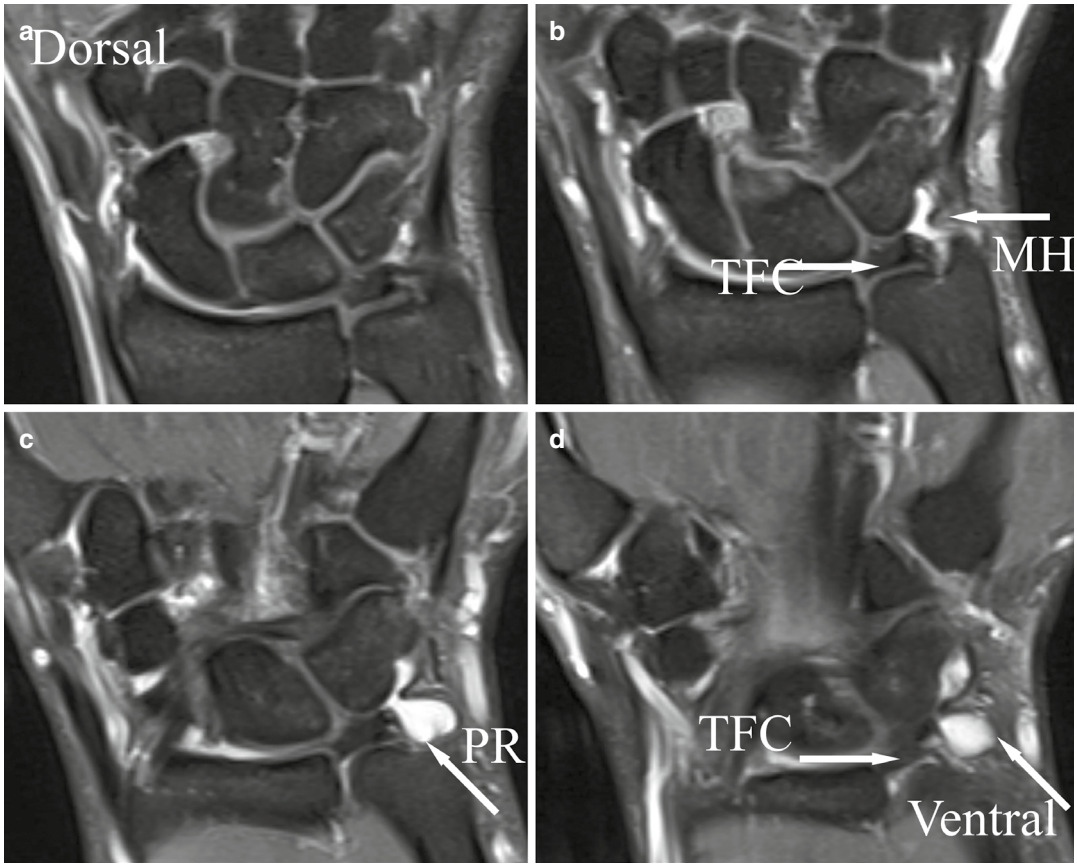

Fig. 45 Ax T2-WI FS (**a**–**d**; from dorsal to ventral). Ventrally, there is a small connection of the RCJ to the prestyloid recess (PR). The meniscus homologue (MH) margins it distally